International Journal of Astrobiology 10 (3): 221–229 (2011)
doi:10.1017/S1473550411000103

Analysis of mineral matrices of planetary soil analogues from the Utah Desert

J.M. Kotler[1], R.C. Quinn[2], B.H. Foing[3], Z. Martins[4] and P. Ehrenfreund[1,5]

[1]*Leiden Institute of Chemistry, Leiden University, 2300 RA Leiden, The Netherlands*
e-mail: jmichellekotler@gmail.com
[2]*Carl Segan Center, SETI institute NASA Ames Research Center, Moffett Field, CA, USA*
[3]*European Space Agency (ESA), ESTEC SRE-S, Postbus 299, 2200 AG Noordwijk, The Netherlands*
[4]*Department of Earth Science and Engineering, Imperial College London, London SW7 2AZ, UK*
[5]*Space Policy Institute, George Washington University, Washington, USA*

Abstract: Phyllosilicate minerals and hydrated sulphate minerals have been positively identified on the surface of Mars. Studies conducted on Earth indicate that micro-organisms influence various geochemical and mineralogical transitions for the sulphate and phyllosilicate minerals. These minerals in turn provide key nutrients to micro-organisms and influence microbial ecology. Therefore, the presence of these minerals in astrobiology studies of Earth–Mars analogue environments could help scientists better understand the types and potential abundance of micro-organisms and/or biosignatures that may be encountered on Mars. Bulk X-ray diffraction of samples collected during the EuroGeoMars 2009 campaign from the Mancos Shale, the Morrison and the Dakota formations near the Mars Desert Research Station in Utah show variable but common sedimentary mineralogy with all samples containing quantities of hydrated sulphate minerals and/or phyllosilicates. Analysis of the clay fractions indicate that the phyllosilicates are interstratified illite–smectites with all samples showing marked changes in the diffraction pattern after ethylene glycol treatment and the characteristic appearance of a solvated peak at ~17 Å. The smectite phases were identified as montmorillonite and nontronite using a combination of the X-ray diffraction data and Fourier–Transform Infrared Spectroscopy. The most common sulphate mineral in the samples is hydrated calcium sulphate (gypsum), although one sample contained detectable amounts of strontium sulphate (celestine). Carbonates detected in the samples are variable in composition and include pure calcium carbonate (calcite), magnesium-bearing calcium carbonate (dolomite), magnesium, iron and manganese-bearing calcium carbonate (ankerite) and iron carbonate (siderite). The results of these analyses when combined with organic extractions and biological analysis should help astrobiologists and planetary geologists better understand the potential relationships between mineralogy and microbiology for planetary missions.

Received 26 January 2011, accepted 9 February 2011, first published online 11 March 2011

Key words: astrobiology, clay minerals, Mars Desert Research Station, Utah.

Introduction

Phyllosilicates occur on Mars since the *in situ* elemental analysis of the Martian surface by the Viking Landers (Toulmin *et al.* 1977), and smectites have been identified in some of the Mars Shergotite, Naklite and Chassigny (SNC) meteorites (Bridges *et al.* 2001; Wyatt & McSween 2002). Mars Express/OMEGA near infrared hyperspectral reflectance data have unambiguously identified nontronite on the Martian surface by its characteristic 2.28 μm absorption band and it is so far the most abundant phyllosilicate detected by the OMEGA instrument (Bibring *et al.* 2006). It has been suggested that the sites where phyllosilicates are preserved on the Martian surface could hold a record of biological molecules, structures or other diagnostic features in the clay-rich surface rocks (Bibring *et al.* 2006). The formation of certain smectites on Earth may be microbially mediated and microbial exudates have been shown to provide favourable nucleation sites for crystal formation (Schultze-Lam *et al.* 1992, 1996a, b). Some researchers also suggest that these clays may have played a significant role in origin of life by providing a substrate for the formation of complex organic molecules (Orofino *et al.* 2010).

Analysis of the mineralogical assignments made by OMEGA and mineralogical data collected by the Mars Exploration Rovers has provided a new geologic model of Martian history based on the abundance of smectite clays (Bibring *et al.* 2005; Poulet *et al.* 2005). From these observations, several conclusions have been made: (1) the deposits in the crust (Syrtis Major, Nili Fossae) predate the volcanism of Syrtis Major, and possibly the formation of the Isidis basin itself; in Marwth Vallis, clay deposits predate Noachian/early Hesperian cratering; (2) the clays are a bulk component of the deposits rather than a surface coating or dust layer; (3) the diversity of the composition indicates that the alteration processes affected the variety of igneous rocks (mafic and Al-rich silicates) constituting the Martian crust (Bibring *et al.* 2005; Poulet *et al.* 2005).

The sequence of geologic alteration events on Mars developed by Bibring *et al.* (2006) shows three sequential eras characterized by the surface alteration products: (1) a non-acidic aqueous alteration traced by phyllosilicates

termed the 'phyllosian' era; (2) an acidic aqueous alteration traced by sulphates termed the 'theiikian' era; and (3) an atmospheric aqueous-free alteration, traced by ferric oxides termed the 'siderikian' era. If this is correct, than the first period in Martian surface evolution (phyllosian) contained an alkaline, possibly moist environment more suitable to life than the later acidic era (theiikian) (Chevrier *et al*. 2007; Mustard *et al*. 2008).

In this paper, we present mineralogical analysis of 10 samples taken in the vicinity of the Mars Desert Research Station (MDRS) near Hanksville, Utah. Samples were collected during the EuroGeoMars 2009 field campaign (Foing *et al*. 2011) from the late Jurassic Morrison formation, the early Cretaceous Dakota Sandstone and the middle cretaceous Mancos Shale (Stoker *et al*. 2011). These formations are characteristic sedimentary deposits containing variable quantities of sands, evaporites and clay minerals with the presence of iron oxides (Chan *et al*. 2004; Ormo *et al*. 2004). The regolith geology and sedimentology of the region have been reported previously (see Clarke & Pain 2004; Battler *et al*. 2006; Clarke & Stoker 2011), but contain geomorphological features dominated by physical processes with complex diagenetic histories that can provide interesting analogue environments for Mars research (Stoker *et al*. 2011). For instance, the Mancos Shale and the Morrison Formation are rich in smectite and sulphate minerals (Nadeau & Reynolds 1981; Clark & Pain 2004) and the Dakota sandstone is composed of mixed, interbedded fine and coarse-grained conglomerate sands containing iron-rich concretions of similar size found by the Mars Exploration Rovers at Meridiani Planum (Battler *et al*. 2006). These mineralogical and geological features along with the arid desert environment at MDRS provide an analogue environment for interdisciplinary planetary science research aimed at characterizing and examining environments that are similar to Mars. The results of the mineralogical analyses of these samples should provide astrobiologists the necessary information to correlate biological and chemical studies of the region (Ehrenfreund *et al*. 2011) to gain a better understanding of potential results from future astrobiology missions to Mars.

Soil sample locations

Experimental section

IR analysis

Spectra were taken using an Excalibur FTS-4000 infra-red spectrometer (BioRad) in the range of 4000–500 cm^{-1} at 2 cm^{-1} resolution. All spectra were background subtracted using a blank KBr pellet spectrum.

X-ray diffraction analysis (XRD)

The samples were analysed on a Philips PW 1830 diffractometer system using Cu Kα radiation, fitted with a PW 1820 goniometer and a graphite monochromator. The generator had the following settings: 45 kV, 40 mA, Hiltonbrooks controlling and output to Traces processing software. The analytical conditions for the whole rock fractions range 2θ (2θ) 2.5°–70°, 0.02° step size and 2 seconds per step; for clays range 2θ 2.5°–40° and 26°, 0.015° step size and 1 second per step.

XRD sample preparation

One gram of sample (whole rock) was crushed in an agate ball mill and back-loaded into a cavity mount before being analysed. For clay analysis, the sample was soaked in distilled water for 24 hours. During this period of time, dispersal using a paddle stirrer or ultrasonic disaggregation was undertaken. Centrifugation was performed when necessary (i.e. presence of salt) to separate the fluid from the dispersed mineral particles (4000 rpm for 20 minutes). The clay was re-suspended in distilled water and centrifuged (1000 rpm for 4 minutes) to produce a suspension of <2 μm. The suspension was then transferred onto a ceramic tile for subsequent XRD analysis.

X-ray photoelectron spectroscopy (XPS) analysis

A subset of the collected samples (P-1, P-2 and P-3) were analysed using X-ray XPS to examine the chemical state of the samples and to verify that the bulk mineralogy (as determined by XRD) is consistent with the chemical state of the sample surfaces. Chemical and physical weathering processes can often result in the alteration of soil and rock surfaces and lead to significant differences from the bulk material (e.g. the formation of desert varnish). In XPS, the energies of

Table 1. *MDRS soil sample locations including coordinates (in decimals of degrees), altitude, depth, the geologic formation and the sample colour*

Sample name	Coordinates	Altitude	Depth	Formation	Colour
P-1	N38.43621° W110.81943°	1350 m	Surface	Mancos Shale/Tunuck	Grey
P-2	N38.40746° W110.7928°	1382 m	Surface	Morrison	White
P-3	N38.40737° W110.7921°	1375 m	Surface	Morrison	Beige pink
P-5	N38.42638° W110.78342°	1400 m	Cliff	Morrison	Rusty pink
P-6	N38.42638° W110.78342°	1400 m	Cliff	Morrison	Green
P-7	N38.45424° W110.79092°	1357 m	Surface	Morrison	Grey pink
P-8	N38.43755° W110.88725°	1482 m	Surface	Mancos Shale	Grey
P-10	N38.43896° W110.89001°	1500 m	Surface	Mancos Shale	Grey
P-13	N38.434063° W110.795470°	1405 m	Surface	Dakota	Light grey
P-14	N38.40630° W110.79547°	1405 m	15 cm	Dakota	Light brown

https://doi.org/10.1017/S1473550411000103 Published online by Cambridge University Press

photoelectrons emitted from a sample that has been irradiated with soft X-rays are measured to determine core-level (1s, 2p, 3d, 4f, etc.) binding energies. Thus, XPS provides detailed chemical bonding information and quantitative elemental analysis from the first 5–10 nm of the surface of the sample. For instance, reduced surface-carbon species can be resolved from increasingly oxidized surface-carbon species based on the energy spectrum of electrons photoejected from the carbon 1s core level in a sample.

Samples were analysed as received from the field site without crushing or grinding. XPS analyses were performed using a Surface Science Instruments spectrometer with a monochromatic Al Kα soft X-ray source (1486.7 eV) with better than 0.5 eV FWHM resolution of XPS core-level spectra. An electron gun set at 0.5 eV, in conjunction with a charging screen place above the sample, was used to minimize surface charging. To account for shifts due to charging effects, peak binding energies were adjusted using a reference value of 284.8 eV for the aliphatic C 1s peak. Survey spectra were collected over a binding energy of 0–1100 eV with a step size of 1 eV. Detailed region spectra were collected with a binding energy step size of 0.1 eV. The error in atom % determination for the major peaks is estimated to be +/−20%.

X-ray diffraction and FT-IR results

Bulk X-ray diffraction (XRD) and 2 μm clay fraction analysis were performed on all samples. The bulk diffraction data results are presented in Table 2. Peak lists for each of the clay mineral analyses are presented in Table 3. FT-IR absorbances are shown in Table 4 with corresponding mineral reference matches indicated for the absorbances. Sample P-1 contains 7% gypsum ($CaSO_4$), 60% quartz (SiO_2), 3% albite ($NaAlSi_3O_8$), trace amounts of K-feldspar (orthoclase-$KAlSi_3O_8$), 7% calcite ($CaCO_3$), 4% dolomite (Ca,Mg$(CO_3)_2$) and 15% total clay minerals. The higher values for albite versus K-feldspar in the plagioclase series indicate a dominance of sodium in the system for the alkali earth elements. The presence of 7% calcite and 4% dolomite in the system are considered common primary minerals in sedimentary formations such as the Morrison shale. The origin of the material is likely biologic and remnant calcified remains of the marine environment present in the Cretaceous North American Inland Sea. The total clay mineral percentage in the samples is 15%. Ethlyene glycol hydration of the 2 μm clay fraction shows a peak shift from the illite (generalized formula-$(K,H_3O)(Al,Mg,Fe)_2(Si,Al)_4O_{10}((OH)_2,(H_2O))$ crystallographic face at 10.13 [001/002] to 17.30 Å, indicating that the sample is a mixed layer of illite–smectite. The FT-IR spectra (absorbances in Table 4, Fig. 1) for P-1 match mineral reference standards both for illite and gypsum indicating that the clay fraction is likely dominated by illite with low quantities of smectite. Corresponding peak absorbances at 3669, 1028 and 525 cm^{-1} match mineral standards for the smectite mineral montmorillonite (generalized formula – $(Na,Ca)_{0.33}(Al,Mg)_2(Si_4O_{10})(OH)_2{\cdot}nH_2O$) (Saha *et al.* 2003).

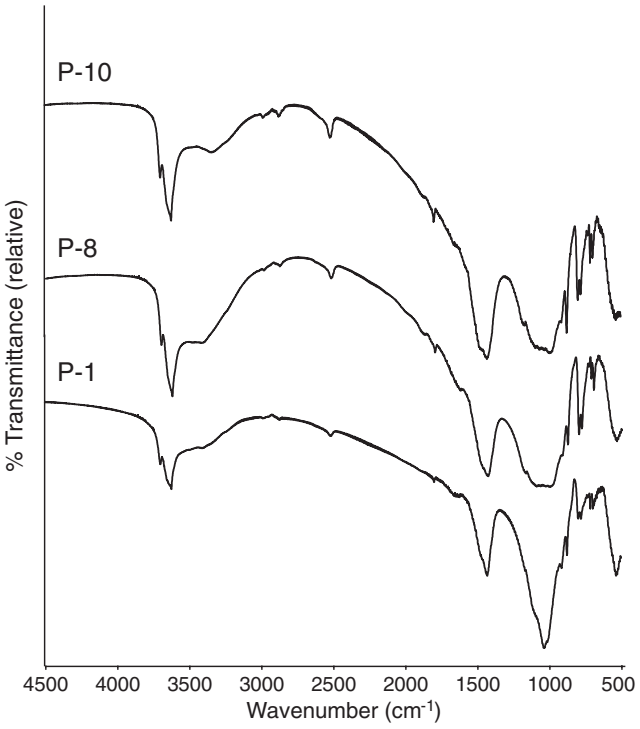

Fig. 1. FT-IR spectra of the Mancos Shale samples P-1, P-8 and P-10, see Table 4 and explanation in the text.

Samples P-8 and P-10 are also from the Mancos Shale. Sample P-8 contains 59% gypsum, 19% quartz, trace amounts of albite, 6% calcite, 2% dolomite, trace amounts of pyrite (FeS_2) and siderite ($FeCO_3$) and 11% total clay (Table 2). Ethlyene glycol hydration of the 2 μm clay fraction shows a peak shift from the illite [001/002] crystallographic face at 10.13 Å to 17.07 Å, indicating that the sample is a mixed layer illite/smectite (see Table 3). Analysis of the FT-IR spectrum of P-8 shows mineral matches for gypsum and illite (Table 4). Identification of the smectite present in the clay fraction is complicated by the presence of absorbances at 3673 and 525 cm^{-1} that are common in the montmorillonite reference spectra, but there is an abundance at 874 cm^{-1} that is common to the nontronite reference spectra. This absorbance is also common to sample P-1 (Fig. 1); however, more spectral evidence for the smectite phase being identified as montmorillonite is suggested by additional absorbances matching montmorillonite in that sample. The presence of pyrite and siderite in the bulk sample would indicate that there is available iron which would suggest that the smectite phase is nontronite $(Ca_{.5}(Si_7Al_8Fe_2)(Fe_{3.5}Al_{.4}Mg_1)O_{20}(OH)_4)$ instead of montmorillonite. Without further analysis, a preliminary phase identification of the smectite phase is inconclusive.

Sample P-10 contains 18% gypsum, 37% quartz, 2% albite, 16% calcite, 4% dolomite, trace amounts of ankerite and 20% total clay (Table 2). Ethlyene glycol hydration of the 2 μm clay fraction shows a peak shift from the illite [001/002] crystallographic face at 10.13 Å to 16.80 Å, indicating that the sample is a mixed layer illite/smectite (see Table 3). The FT-IR

https://doi.org/10.1017/S1473550411000103 Published online by Cambridge University Press

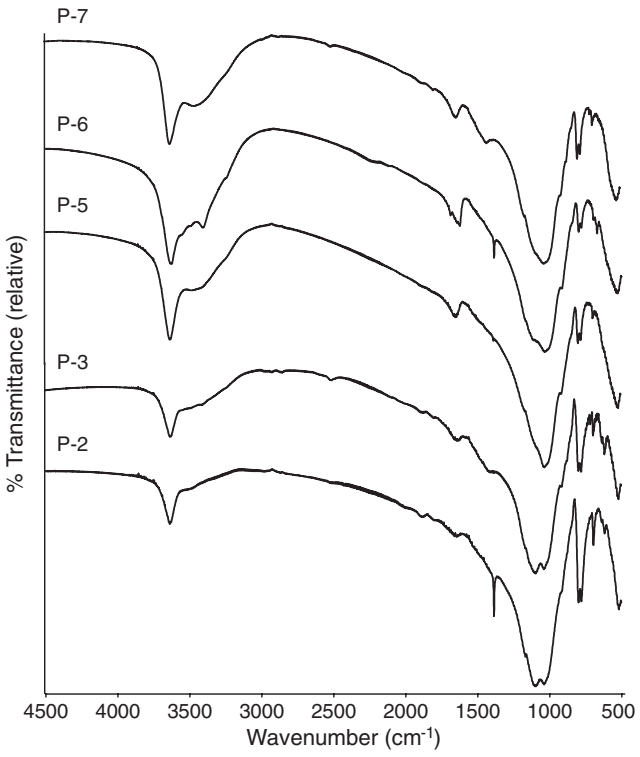

Fig. 2. FT-IR spectra of the Morrison Formation samples P-2, P-3, P-5, P-6 and P-7. See Table 4 and explanation in the text.

spectrum for P-10 shows strong matches to mineral reference abundances for illite and gypsum (Table 4). Similar to both PE-1 and PE-8, there is an abundance match at 874 cm^{-1} that correlates to the nontronite reference spectrum. However, the other abundances that correlate to montmorillonite at 3670 and 525 cm^{-1} are also present. Without the presence of iron-bearing phases in the bulk X-ray diffraction data (Table 2), an identification of the smectite phase as montmorillonite is likely conclusive.

Samples P-2, P-3, P-5, P-6 and P-7 were collected in the Morrison Formation (late Jurassic). Sample P-3 contains 6% gypsum, 46% quartz, 24% albite, trace levels K-feldspar, 2% calcite 1%, celestine, trace amounts of ankerite and 18% total clay (Table 2). The higher values for albite versus K-feldspar indicate a dominance of sodium in the system for the alkali earth elements. Ethlyene glycol hydration of the 2 μm clay fraction shows a peak shift from the illite [001/002] crystallographic face at 8.76 Å to 16.70 Å, indicating that the sample is a mixed layer of illite–smectite (see Table 3). The FT-IR spectrum of P-3 shows a strong correlation to reference spectra for both illite and montmorillonite indicating that the clay fraction is likely a mixed layer illite/montmorillonite (Table 4, Fig. 2).

Sample P-5 contains high levels of quartz (73%), trace levels of K-feldspar, 1% calcite, traces levels of ankerite, trace levels of hematite and 23% total clay (Table 2). Ethlyene glycol hydration of the 2 μm clay fraction shows a peak shift from the illite [001/002] crystallographic face at 10.13 Å to 16.73 Å, indicating that the sample is a mixed layer of illite/smectite (see Table 3). The FT-IR spectra for P-5 contains peaks with overlapping abundances between both montmorillonite and nontronite with only one separate characteristic peak that is close is absorbance to gypsum (Table 4, Fig. 2). Given that the bulk XRD did not identify gypsum in P-5, it is likely that the smectite present in the clay fraction is nontronite $(Ca_{.5}(Si_7Al_{.8}Fe_{.2})(Fe_{3.5}Al_{.4}Mg_{.1})O_{20}(OH)_4)$. Additionally, the bulk XRD showed the presence of trace levels of ankerite and hematite which are both iron-bearing mineral phases indicating the likelihood of trivalent iron in the mineral formula.

Sample P-6 contains 14% gypsum, 46% quartz, 2% albite, trace amounts of K-feldspar, dolomite, pyrite and 33% total clay. Ethlyene glycol hydration of the 2 μm clay fraction shows a peak shift from the illite [001/002] crystallographic face at 10.13 Å to 16.90 Å, indicating that the sample is a mixed layer of illite–smectite (see Table 3). The FT-IR spectrum shows similar peak abundances to P-5 with overlap on indicator peaks making a clear identification of the smectite mineral phase difficult because P-6 contains gypsum and lacks some of the key montmorillonite peaks found in several of the other samples (Table 4, Fig. 2). The presence of pyrite in the samples does indicate that available divalent iron could be present in the system, which could be oxidized to provide the trivalent iron needed to form nontronite during diagenesis. Without further analysis, however, a clear identification is not possible and the clay fraction can only be characterized as a mixed layer illite/smectite.

Sample P-7 contains 61% quartz, 6% albite, 3% K-feldspar, 19% calcite, 1% ankerite, 1% hematite, 1% siderite and 6% total clay (Table 2). Ethlyene glycol hydration of the 2 μm clay fraction shows a peak shift from the illite [001/002] crystallographic face at 10.13 Å to 16.73 Å, indicating that the sample is a mixed layer illite/smectite (see Table 3). The FT-IR spectrum of P-7 shows a strong correlation with absorbances for the illite standard and montmorillonite standard spectra indicating that the clay fraction is a mixed layer of illite/montmorillonite (Table 4, Fig. 2). The presence of hematite and siderite in the sample would indicate that there is available oxidized iron in the whole rock; however, the FT-IR spectrum shows a stronger match for montmorillonite than nontronite.

Sample P-2 contains 78% quartz, 3% albite, 1% K-feldspar, trace amounts of ankerite and 16% total clay (Table 2). Ethlyene glycol hydration of the 2 μm clay fraction shows a peak shift from the illite [001/002] crystallographic face at 8.86 Å to 16.59 Å, indicating that the sample is a mixed layer illite/smectite (see Table 3). Comparison of the FT-IR spectrum with the reference standards indicates that the clay fraction is composed of a mixed layer of illite/montmorillonite (Table 4, Fig. 2). The lack of iron-bearing mineral phases in the sample supports the conclusion that the smectite is montmorillonite instead of nontronite.

Samples P-13 and P-14 were collected from the Dakota Sandstone (late Cretaceous) from two separate locations (Table 1). Sample P-13 contains 68% quartz, 3% albite, 2% K-feldspar, trace amounts of ankerite and 9% total clay (Table 2). Ethlyene glycol hydration of the 2 μm clay fraction

https://doi.org/10.1017/S1473550411000103 Published online by Cambridge University Press

Table 2. *Bulk XRD results of the MDRS samples. Sample names and geologic formation are indicated: (MS), Mancos Shale; (M), Morrison Formation; (DS), Dakota Sandstone*

Mineral	P-1 (MS)	P-2 (M)	P-3 (M)	P-5 (M)	P-6 (M)	P-7 (M)	P-8 (MS)	P-10 (MS)	P-13 (DS)	P-14 (DS)
Gypsum ($CaSO_4{\cdot}2H_2O$)	7		6		14		59	18		73
Quartz (SiO_2)	60	78	46	73	46	61	19	37	68	14
Albite ($NaAlSi_3O_8$)	3	3	24		2	6	<1	2	3	
K-feldspar ($KAlSi_3O_8$)	<1	1	<1	<1	<1	3			2	
Calcite ($CaCO_3$)	7		2	1		19	6	16	15	1
Dolomite ($CaMg(CO_3)_2$)	4				<1		2	4	<1	10
Total clay	15	16	18	23	33	6	11	20	9	1
Celestine ($SrSO_4$)			1							
Ankerite ($Ca(Fe, Mg, Mn)(CO_3)_2$)		<1	<1	<1		1				
Hematite (Fe_2O_3)				<1		1				
Pyrite (FeS_2)					<1		<1			
Siderite ($FeCO_3$)						1	<1	<1		<1

shows a peak shift from the illite [001/002] crystallographic face at 8.82–16.88 Å, indicating that the sample is a mixed layer of illite–smectite (see Table 3). The FT-IR spectrum for P-13 shows strong correlation with the illite reference spectrum (Table 4). Abundance matches with the nontronite reference spectra occur at 1026 and 873 cm^{-1} indicating that the smectite phase is likely nontronite. Therefore, the clay fraction is composed of a mixed layer of illite/nontronite phase.

Sample PE-14 contains 78% gypsum, 14% quartz, 1% calcite, 10% dolomite, trace amounts of siderite and 1% total clay (Table 2). The total clay percentage was only 1% making XRD analysis of the clay fraction problematic. The XRD pattern of the clay fraction was not indicative of clay minerals and was dominated by small crystallites of quartz (data not shown). Therefore, identification of the clay fraction was not completed for this sample. The FT-IR spectrum for P-14 shows a strong correlation to the reference spectrum for gypsum (Table 4, Fig. 3). There are peak abundance matches for illite at 1417 and 775 cm^{-1} and also a match for montmorillonite at 525 cm^{-1}; however, given the low abundance of clay in the total sample, the identification of the clay mineral phase was omitted.

XPS results

Table 5 shows the atom % elemental surface composition of samples P-1, P-2 and P-3 as determined from survey spectra. The average elemental composition of each of three samples is similar and consistent with the bulk compositions as determined by XRD analysis and presence of aluminosilicates as major components. There are a few minor differences in elemental composition between the samples, most notably, the lack of detectable sulphur in the P-1 sample. The binding energy of the sulphur in samples P-2 and P-3 is consistent with the presence of sulphate and the calcium-binding energies in samples P-1 and P-3 is consistent with the presence of gypsum. Potassium was not detected in samples P-2 and P-3 and calcium was not detected in sample P-2. The variability in compositions between samples and as reflected in comparisons of the XRD and XPS dataset can be explained by the low sensitivity of XPS to the minor components, sample heterogeneity and the sample preparation methods. While the XRD samples were ground and homogenized prior to sample analysis, the XPS samples were analysed as is to avoid surface alteration.

Variations in levels of surface carbon were observed, with the lowest value (16.9%) for the P-1 sample and the largest value for the P-3 sample (24.5%). The presence of significant levels of adventitious carbon on sample surfaces is expected. However, detailed analysis of the C 1s region can yield insight into the chemical state, including the extent of oxidation, of carbon on the surface of the sample. Figure 4 shows high-resolution, C 1s core-level spectra for samples P-1, P-2 and P-3. Carbonate is a minor component in all samples and the levels of oxidized carbon are relatively uniform across all samples. The overall lower level of surface carbon in sample P-1 can be attributed to lower levels of reduced carbon relative to samples P-2 and P-3.

Discussion

Proposed landing sites for future exploration of Mars including the NASA Mars Science Laboratory (MSL) mission scheduled to launch in 2011 include regions that are rich in phyllosilicate smectite clay minerals such as nontronite, montmorillonite and saponite (Rogers & Bandfield 2009). Therefore, the presence of these mineral phases in an analogue site such as those at MDRS correlated to astrobiology studies (Ehrenfreund *et al.* 2011) can potentially reveal the types of minerals to target for future missions.

All of the samples in this study contained mixed layer illite/smectites as confirmed by X-ray diffraction and FT-IR analysis (Tables 3 and 4). Mixed layer illite/smectites are much more common than discrete illite or smectite on Earth (Moore & Reynolds 1997); however, little attention has been given to finding mixed-layer clays on Mars. For instance, on Mars, different phyllosilicates can be found in close proximity to one another. Data from Mawrth Vallis provided by OMEGA and CRISM provide evidence for the presence of outcrops rich in Fe/Mg smectites and montmorillonite, while

https://doi.org/10.1017/S1473550411000103 Published online by Cambridge University Press

Table 3. *MDRS clay fraction XRD peak positions. The 001* EG smectite crystallographic face represents diffraction analysis after ethylene glycolation. Sample names and geologic formation are indicated: (MS), Mancos Shale; (M), Morrison Formation; (DS), Dakota Sandstone*

	001* EG smectite		001/002 illite		002/003 illite	
Sample	*d* (Å)	° 2 θ	*d* (Å)	° 2 θ	*d* (Å)	° 2 θ
P-1 (MS)	17.30	5.11	10.13	8.80	5.03	17.68
P-2 (DS)	16.59	5.32	8.86	10.90	5.57	15.90
P-3 (M)	16.70	5.29	8.76	10.75	5.62	15.85
P-5 (M)	16.73	5.28	10.13	8.80	5.57	15.91
P-6 (M)	16.90	5.20	10.13	8.80	5.59	15.82
P-7 (M)	16.73	5.28	10.13	8.80	5.06	17.56
P-8 (MS)	17.07	5.17	10.13	8.82	5.01	17.68
P-10 (MS)	16.80	5.23	10.13	8.80	5.00	17.62
P-13 (DS)	16.88	5.07	10.13	8.82	5.07	17.47

CRISM data from Nili Fossae provide evidence for the presence of limited outcrops rich in high-Fe chlorite, kaolinite and muscovite/illite (Mustard *et al.* 2008). Rampe *et al.* (2008) suggests the possibility of mixed-layer clays on Mars; however, with this exception current literature does not address the inherent analytical challenges related to identifying mixed-layer clays. In particular, challenges related to remote robotic planetary sample analysis of mixed-layer clays. Additionally, Bish & Vaniman (2008) suggest that the presence of smectites in Noachian terrains on Mars could substantially alter our understanding of the stability of clay mineral phases. For example, our understanding of the stability of smectites and mixed-layer clays is dependent on stability relationships with illite being the more stable high-temperature phase, which should subsist for longer periods in the geologic record. Therefore, the absence of mixed-layer clays on Mars in Noachian terrains could rewrite our understanding of clay mineral stability and suggests that, in the absence of (plate) tectonic activity and burial, 'metastable' clay minerals may be 'stable' for times of the order of the age of our planet (Bish *et al.* 2003; Bish & Vaniman 2008).

It has been suggested that the formation of some smectites on Earth may be microbially mediated and that microbial exudates provide favourable nucleation sites for crystal formation (Schultze-Lam *et al.* 1992, 1996a, b). Other researchers have found that microbes significantly contribute to the smectite–illite reaction that is an important mineral reaction during sediment diagenesis (Kim *et al.* 2004, Zhang *et al.* 2007). Formation mechanisms for nontronite on the sea floor include the alteration of volcanic rock fragments and glasses, low-temperature reaction of Fe-hydroxides with biogenic silica and direct precipitation from hydrothermal fluids (Cole & Shaw 1983). From this mechanism it has been suggested that nontronite formation can be biologically mediated (Ueshima & Tazaki 2001). Morphology of nontronite samples taken from the sea floor are ordered spheroids or tubes a few μm in diameter, similar to that of microbial structures (Kohler *et al.* 1994; Fortin *et al.* 1998). The work of Schultze-Lam *et al.* (1992, 1996a, b) has shown that polymeric substances exuded from microbial cells such as the S-layer, mucopolysaccarides, capsules and other biomolecules often provide nucleation sites and/or favour a chemical microenvironment suitable for biomineralization.

Recent studies have also indicated that microbes may play a role in the smectite to illite reaction (Kim *et al.* 2004; Zhang *et al.* 2007). When the water bearing and expandable smectite is buried and subject to increasing temperature and pressure, the smectites tend to transform to illite (Dong *et al.* 1997; Dong 2005). The smectite to illite reaction (S–I) is an important mineral reaction during sediment diagenesis of mudstones and shales (Peacor 1992), as the degree of reaction termed 'smectite illitization' is linked to maturation, migration and trapping of hydrocarbons (Weaver 1960; Burst 1969; Pevear 1999). Smectite illitization is also used in the development of pore pressures (Freed & Peacor 1989), growth faults (Bruce 1984), rock cementation and porosity reduction (Boles & Franks 1979; Bjorkum & Nadeau 1998) and pore water chemistry (Brown *et al.* 2001). In the absence of microbial activity reaction conditions usually require parameters of 300–350 °C , 100 MPa and 4 to 5 months (Zhang *et al.* 2007). However, Kim *et al.* (2004) found that in the presence of microbes the reaction can take place at room temperature and one atmosphere pressure within 2 weeks. During the microbial-mediated reaction Zhang *et al.* (2007) demonstrated a strong catalytic effect from the organic matter trapped in the smectite structure aiding in the illite transition. It is thought that during the microbial formation process smectite may be partially dissolved, and illite precipitated with the extent of microbial dissolution depending on factors such as the amount of Fe^{3+} in the structure and its site occupancy, type of bacteria, solution chemistry and temperature conditions (Zhang *et al.* 2007).

Overall, the smectites are an interesting mineral group that plays roles in several aspects of geology and geochemistry. Understanding nontronites' physico-chemical properties allows researchers to better understand surface and subsurface processes on both Earth and potentially Mars. The iron-rich smectite nontronite possesses crystallographic properties that allow the understanding of hydration states and environmental conditions present during formation. A critical involvement in biomineralization, biosignature storage and catalytic activity associated with microbially activity makes the study of nontronite attractive for astrobiological investigations.

Smectites and illites

The smectite to illite transition (S–I) can be a powerful tool to assess the thermal maturity for organic matter in sedimentary basins. Water held in the expandable layer of smectites is released as the mineral is transformed to illite (non-expandable). The amount of water and organic matter available in the pore spaces and interstial sites could be important for the search for life on Mars. In the exploitation of natural resources on Earth, such as oil exploration, these transitions have been studied extensively (Moore & Reynolds 1997). However, the role these transitions play on Mars needs to be carefully considered when potential astrobiology sites are selected. The

https://doi.org/10.1017/S1473550411000103 Published online by Cambridge University Press

Table 4. *MDRS FT-IR sample absorbances (cm^{-1}) and corresponding vibration mode. Sample names and geologic formation are indicated: (MS), Mancos Shale; (M), Morrison Formation; (DS), Dakota Sandstone*

Reference mineral reference absorbance	Sample absorbance (cm^{-1})									
	P-1 (MS)	P-2 (M)	P-3 (M)	P-5 (M)	P-6 (M)	P-7 (M)	P-8 (MS)	P-10 (MS)	P-13 (DS)	P-14 (DS)
Montmorillonite[a]	3669						3673	3670	3695	
Illite[b]	3620	3631	3623	3624	3620	3621	3620	3620	3620	
										3546
Illite[b]						3422				
Gypsum[d]					3396		3393			3397
								3313		
Illite[b]							2510	2510		
Gypsum[d]										2218
								1797		
Illite[b], Montmorillonite[a], Nontronite[c], Gypsum[d]				1637	1621	1631				1620
Illite[b]	1426					1416	1428	1421	1427	1417
		1383			1383					
Montmorillonite[a]		1083	1088							1109
Gypsum[d], Nontronite[c]	1028	1026	1027	1018	1017	1009	1006	1006	1026	
Nontronite[c]	874						874	873	873	872
Illite[b]	776	775	776	776	778	778	778	776	776	775
Illite[b]	694	693	693	693		693	694	694	694	
Gypsum[d]										667
Montmorillonite[a]			614		637					
										598
Montmorillonite[a]	525				524		525	525	525	525
		515	515	514		516				

[a] Montmorillonite reference spectrum (Saha *et al*. 2003).
[b] Illite reference spectrum (Hermosin & Perez Rodriguez 1981).
[c] Nontronite reference spectrum (Frost *et al*. 2002).
[d] Gypsum reference spectrum (Seidl & Knop 1969).

analytical challenges of determining the ratio of illite to smectite and determining the exact smectite mineral phase can be a daunting task and requires careful laboratory preparation of samples on Earth. For instance, in this study, the clay fractions are separated from the bulk material (2 μm clay fraction) and subjected to sample preparation techniques to aid in identification. In order to obtain high-quality X-ray diffraction data, samples must be as mineralogically homogeneous as possible. Careful sample preparation is critical to obtaining quantitative data such as that which can determine the ratio of illite to smectite. In theory, a comparison of the air-dried and ethylene glycol solvated samples (see Table 3) would give a value known as the °Δ2θ, which is a sensitive indicator both for the degree of ordering in the sample (Reichweite) and the percent composition. In the case where samples potentially contain discrete illite and interstratified illite smectites, which are common in terrestrial shales, these additional quantitative assessments can be difficult to make. This type of information could be very valuable in astrobiological studies of Mars because the expandable layers in the smectites have a high cation exchange potential and also can provide water and organic matter to facilitate microbial growth and survival. Given the inherent analytical challenges for identifying and quantifying the degree of illitization in a clay fraction in terrestrial settings, extensive work and understanding of the effect of mixed-layer clays and their effect on the detection of organic matter and/or microbial life for Mars applications need to be undertaken for future studies.

Fig. 3. FT-IR spectra of the Dakota Formation samples P-13 and P-14. See Table 4 and explanation in the text.

Organics and minerals

Identifying the types of organic molecules that may be associated with the smectites clays, interstratified mixed clay samples and other types of clay samples that may be encountered on the Martian surface using instruments

https://doi.org/10.1017/S1473550411000103 Published online by Cambridge University Press

Table 5. *XPS elemental composition (atom %)*

Element	P-1	P-2	P-3
Na	1.6	7.1	5.4
Fe	0.6	0.8	0.4
Mn	0.2		
O	55.9	52.7	49.7
Ca	0.9		0.6
K	0.5		
C	16.9	18.4	24.4
Cl	0.5	0.3	0.4
S		2.4	1.4
Si	12.5	10.9	9.7
Al	8.5	5.7	5.3
Mg	2.3	2.3	2.6

currently scheduled to explore the Martian surface are key goals for astrobiologists. In particular, the types of biosignatures that may be encountered during the MSL mission to clay-rich sites on Mars are a high priority. By analysing the types of organic molecules and/or biosignatures that are found in analogue environments on Earth mission researchers will be able to better interpret and develop data analysis techniques for the upcoming missions to ensure mission success. This includes studies such as those conducted at the MDRS site in analogue environments where a variety of mineralogical microenvironments can be encountered and studied. Mineralogical analysis of the Mancos Shale for instance, showed variable quantities for nearly all of the major mineral groups (Table 2). All of the samples contained secondary mineralization with variable quantities of gypsum, quartz, calcite and clay content. The same heterogeneity is observed in samples from the Morrison formation and the Dakota Sandstone. XPS data for samples P-1 (Mancos Shale), P-2 and P-3 (Morrison formation) show variable elemental values for all of the samples. Significant variations in elemental and mineralogical compositions are observed for samples collected over relatively small distances during the EuroGeoMars 2009 campaign. Likewise, diverse geological environments have been discovered by the MER Spirit and Opportunity rovers over comparable distances.

Perspectives

Correlation and integration of the mineralogy results in the astrobiology context for the samples examined at the MDRS field site (Ehrenfreund *et al.* 2011; Martins *et al.* 2011) suggest high levels of clay could be problematic for the detection of organic molecules by the techniques used, this could be due to several factors including adsorption, intercalation and trapping of organic matter in expandable clay minerals that is difficult to remove. The removal of organic compounds from clay samples is a common process used to improve the quality and allow quantification of X-ray diffraction data because the presence of organic matter can cause broad diffraction peaks. The techniques typically used involved complete oxidation and removal of the organic compounds using alkaline hydrogen peroxide solutions, heating and centrifugation. It is therefore important for future studies that address organic interactions

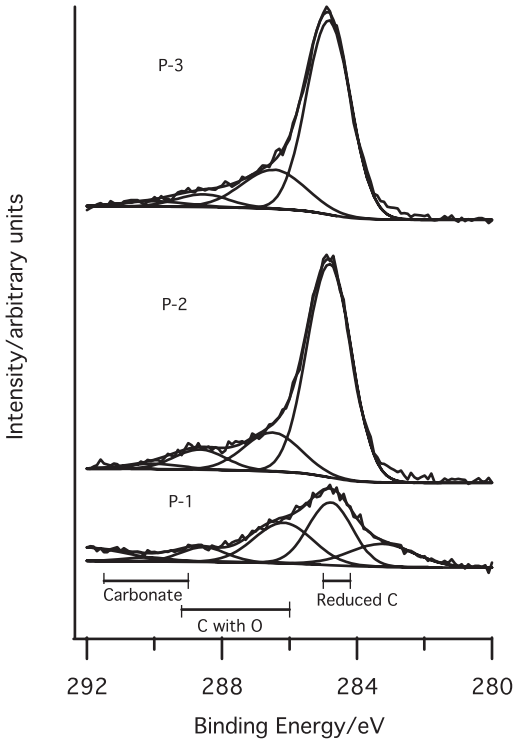

Fig. 4. High-resolution XPS C 1s core-level spectra for samples P-1, P-2 and P-3.

with clay materials to utilize and optimize the extraction of organic matter from clay materials. Specifically, analysing the clay fraction separately from the bulk material may lead to a better understanding of how to specifically extract organic matter from these mineral phases. Alternative extraction solutions should be explored so that the supernatant can be analysed and could provide identification of the original state of the organic matter, which is important for astrobiology studies. Alternately, direct laser desorption studies of the clay fractions could circumvent the issues related to extraction procedures and could be viable for space flight (Kotler *et al.* 2008). Understanding the instrumental limitations and correlating these data with geological analogue sites such as MDRS (Foing *et al.* 2011) will allow a better understanding of the types of molecules that can be identified and will help guide future missions to explore Mars for the presence of extant and or extinct life.

Acknowledgements

Pascale Ehrenfreund was supported by the NASA Astrobiology Institute (NAI). Zita Martins was supported by the Royal Society. Zita Martins acknowledge the Science and Technology Facilities Council (STFC) for financial support. The EuroGeoMars 2009 campaign was organized and supported by the International Lunar Exploration working Group (ILEWG), NASA Ames Research Centre and ESA/ESTEC. We acknowledge the contribution of the EuroGeoMars 2009 campaign crew and the mission support team. This research was conducted in the framework of the

Mars Express Recognized Cooperating Laboratory for geochemistry.

References

Battler, M.M., Clarke, J.D.A. & Coniglio, M. (2006). Implications for Martian field studies. In *Mars Analog Research*, ed. Clarke, J.D.A., pp. 55–70. American Astronautical Science and Technology Series 111. Univiet Publishers, San Diego, California, USA.

Bibring, J.P., Langevin, Y., Gendrin, A., Gondet, B., Poulet, F., Berthe, M., Soufflot, A., Arvidson, R., Mangold, N., Mustard, J. *et al.* (2005). *Science* **307**, 1576–1581.

Bibring, J.P., Langevin, Y., Mustard, J.F., Poulet, F., Arvidson, R., Gendrin, A., Gondet, B., Mangold, N., Pinet, P., Forget, F. *et al.* (2006). *Science* **21**, 400–404.

Bish, D.L., Carey, J.W., Vaniman, D.T. & Chipera, S.J. (2003). *Icarus* **164**, 96–103.

Bish, D.L. & Vaniman, D.T. (2008). Workshop on Martian Phyllosilicates: Recorders of Aqueous Processes? held 21–23 October 2008 in Paris, France. LPI Contribution No. 1441, p. 17–18.

Bjorkum, P.A. & Nadeau, P.H. (1998). *APPEA J*. **38**, 453–464.

Boles, J.R. & Franks, S.G. (1979). *J. Sedimentary Pet*. **49**, 55–70.

Bridges, J.C., Catling, D.C., Saxton, J.M., Swindle, T.D., Lyon, I.C. & Grady, M.M. (2001). *Space Sci. Rev*. **96**, 365–392.

Brown, K.M., Saffer, D.M. & Bekins, B.A. (2001). *Earth Planet. Sci. Lett.* **194**, 97–109.

Bruce, C.H. (1984). *Am. Assoc. Pet. Geol. Bull*. **53**, 73–93.

Burst, J.F. (1969). *Am. Assoc. Pet. Geol. Bull*. **53**, 73–93.

Chan, M.A., Beitler, B., Parry, W.T., Ormo, J. & Komatsu, G. (2004). *Nature* **429**, 731–734.

Chevrier, V., Poulet, F. & Bibring, J.-P. (2007). *Nature* **448**, 60–63.

Clarke, J. & Stoker, C. (2011). *Int. J. Astrobiol*. **10**, 161–175.

Clarke, J.D.A. & Pain, C.F. (2004). *Am. Astronaut. Sci. Technol. Ser*. **107**, 131–160.

Cole, T.G. & Shaw, H.F. (1982). *Clay Miner*. **18**, 239–252.

Dong, H. (2005). *Clay Sci*. **12** (Suppl. 1), 6–12.

Dong, H., Peacor, D.R. & Freed, R.L. (1997). *Am. Miner*. **82**, 379–391.

Ehrenfreund, P., Röling, W., Thiel, C., Quinn, R., Septhon, M., Stoker, C., Direito, S., Kotler, M., Martins, Z., Orzechowska, G.E. *et al.* (2011). *Int. J. Astrobiol*. **10**, 239–253.

Foing, B., Stoker, C., Zavaleta, J., Ehrenfreund, P., Thiel, C., Sarrazin, P., Blake, D., Page, J., Pletser, V., Hendrikse, J., *et al.* (2011). *Int. J. Astrobiol*. **10**, 141–160.

Fortin, D., Ferris, F.G. & Scott, S.D. (1998). *Am. Mineral.* (In press) **83**, 1399–1408.

Freed, R.L. & Peacor, D.R. (1989). *Am. Assoc. Pet. Geol. Bull*. **73**, 1223–1232.

Frost, R.L., Kloprogge, J.T. & Ding, Z. (2002). *Spectrochim. Acta Part A – Mol. Biomol. Spectrosc*. **58**, 1657–1668.

Hermosin, M.C. & Perez Rodriguez, J.L. (1981). *Clays Clay Miner*. **29**, 143–152.

Kim, J.W., Dong, H., Seabaugh, J., Newell, S.W. & Eberl, D.D. (2004). *Science* **303**, 830–832.

Kohler, B., Singer, A. & Stoffers, P. (1994). *Clay Miner*. **42**, 689–701.

Kotler, J.M., Hinman, N.W., Scott, J.R., Yan, B. & Stoner, D.L. (2008). *Astrobiology* **8**, 253–266.

Martins, Z., Sephton, M.A., Foing, B.H. & Ehrenfreund, P. (2011). *Int. J. Astrobiol*. **10**, 231–238.

Moore, D.M. & Reynolds, R.C. (1997). *X-Ray Diffraction and the Identification and Analysis of Clay Minerals*. Oxford University Press, New York, 378 pp.

Mustard, J.F., Murchie, S.L., Pelkey, S.M., Ehlmann, B.L., Milliken, R.E., Grant, J.A., Bibring, J.-P., Poulet, F., Bishop, J., Dobrea, E.N. *et al.* (2008). **454**, pp. 305–309.

Nadeau, P.H. & Reynolds, R.C. (1981). *Clays Clay Miner*. **29**, 249–259.

Ormo, J., Komatsu, G., Chan, M.A., Beitler, B. & Parry, W.T. (2004). *Icarus* **171**, 295–316.

Orofino, V., Blanco, A., D'Elia, M.D., Licchelli, D., Font, S. & Marzo, G.A. (2010). *Icarus* **208**, 202–206.

Peacor, D.R. (1992). In *Reviews in Mineralogy: Minerals and Reactions at the Atomic Scale: Transmission Electron Microscopy*, ed. Buseck, P.R., vol. 27, pp. 335–380. BookCrafters Inc., Chelsea.

Pevear, D.R. (1999). *Proc. Natl Acad. Sci. U.S.A.* **96**, 3440–3446.

Poulet, F., Bibring, J.-P., Mustard, J.F., Gendrin, A., Mangold, N., Langevin, Y., Arvidson, R.E., Gondet, B. & Gomez, C. (2005). *Nature* **438**, 623–627.

Rampe, E.B., Kraft, M.D., Sharp, T.G., Williams, L. & Turner, A. (2008). *American Geophysical Union, Fall Meeting 2008*, abstract #P53B-1444.

Rogers, A.D. & Bandfield, J.L. (2009). *Icarus* **203**, 437–453.

Saha, U.K., Iwasaki, K. & Sakurai, K. (2003). *Clays Clay Min*. **51**, 481–492.

Schultze-Lam, S., Harauz, G. & Beveridge, T.J. (1992). *J. Bacteriol*. **174**, 7971–7981.

Schultze-Lam, S., Ferris, F.G., Sherwood-Lollar, B. & Gerits, J.P. (1996a). *Can. J. Microbiol*. **42**, 147–161.

Schultze-Lam, S., Fortin, D. & Beveridge, T.J. (1996b). *Chem. Geol*. **132**, 171–181.

Seidl, V. & Knop, O. (1969). *Can. J. Chem*. **47**, 1361–1368.

Stoker, C., Clarke, J., Direito, S., Martin, K., Zavaleta, J., Blake, D. & Foing, B.H. (2011). *Int. J. Astrobiol*. **10**, 269–289.

Toulmin, P., Baird, A.K., Clark, B.C., EKil, K., Rose, H.J., Evans, P.H. & Kelliher, W.C. (1977). *J. Geophys. Res*. **82**, 4625–4634.

Ueshima, M. & Tazaki, K. (2001). *Clays Clay Min.* **49** (4), 292–299.

Weaver, C.E. (1960). *Am Assoc. Pet. Geol*. **44**, 1505–1518.

Wyatt, M.B. & McSween, H.Y. (2002). *Nature* **417**, 263–266.

Zhang, G., Kim, J., Dong, H. & Andre, J.S. (2007). *Am. Mineral*. **92**, 1401–1410.